# Robotic Fish Based on a Polymer Actuator

**Han Wang, Sungkono Surya Tjahyono, Bruce MacDonald, Paul A. Kilmartin, Jadranka Travas-Sejdic, and Rudolf Kiefer**
**Department of Electrical and Computer Engineering**
**And**
**Polymer Electronic Research Centre**
**University of Auckland, New Zealand**
hwan122, stja001@ec.auckland.ac.nz, b.macdonald, p.kilmartin, j.travas-sejdic, r.kiefer@auckland.ac.nz

## Abstract

Conducting polymer (CP) materials exhibit significant volume change in response to electrical stimulation. In this paper we present a polymer actuated biomimetic robotic fish. The robot is propelled by a trilayer polypyrrole (PPy) polymer actuator. Experiments were conducted to characterize the properties of PPy polymer. Different configurations of actuators were investigated and justified using experimental results. The robotic fish embeds a microcontroller, a Lithium coin cell battery, and necessary circuitry for navigation and control. It cruises using the actuated tail fin. Waterproofing packaging is designed to protect the electronics. This project has successfully demonstrated that PPy polymers can be used to design robotic fish actuators. A self-contained prototype is demonstrated with 10~12 hours operation lifetime.

## 1 Introduction

Natural muscles are highly effective and power-efficient actuators introduced through millions of years of biological evolution. The elegant and gentle movements of natural muscles have not been reproduced by man-made devices [Reynolds 2006]. Scientists have been looking for a technology capable of emulating the behavior and performance of real muscles. Conducting polymers (CPs) are a class of Electroactive polymers (EAP) that exhibit shape change in response to electrical stimulation have made these materials an attractive candidate for artificial muscles [Bar-Cohen 2001; Bar-Cohen 2004].

Fish-like robots can be propelled by EAP based actuators. Robotic fish have wide potential for application, ranging from ocean investigation [Leonard and Graver 2001] and defense [Bandyopadhyay 2005] at the meter scale, to smart toy fish at the centimeter scale [Bar-Cohen 2004], to micro-surgery at the millimeter to micrometer scale [Edd, Payen et al. 2003]. EAP based actuators have been explored at millimeter to centimeter scale due to their low power consumption [Punning, Anton et al. 2004], high energy conversion efficiency and noiseless operation [Tan, Kim et al. 2006].

Generally, EAPs can be divided into two major groups depending on their activation mechanism: ionic and electronic [Bar-Cohen 2004]. The electronic EAPs, such as piezoelectric, electrostatic, or ferroelectric materials, work under the influence of an applied electric field. These materials have the advantages of rapid response, high mechanical energy density and retainable strain under dc activation [Bar-Cohen 2004]. In contrast, ionic EAPs, such as conductive polymers, requires low voltage for actuation, typically ± 1V [Smela 2003]. The moderate strain (1-3%), high strength (1000 times as great as skeletal muscle) and low weight make CPs particularly well suited for biomimetic applications [Spinks, Liu et al. 2002; Smela 2003; Kiefer, Paul A. Kilmartin et al. 2007].

Polypyrrole (PPy) and polyaniline (PANI) are the most widely studied CPs, because of their good chemical stability and substantial strains. PPy polymers undergo volumetric change as they are oxidized and reduced [Kiefer, Paul A. Kilmartin et al. 2007]. Recent work on polymer actuator design has used this volumetric change to generate bending motions. A robotic fish propelled by pectoral fins has been developed in University of Wollongong to demonstrate this concept [Alici and Spinks 2006].

In this paper, the development of a tail cruising robotic fish is presented. This is the first time that a self-powered and PPy actuated biomimetic swimming robot is demonstrated. This is achieved by designing a fish body with battery and electronic circuitry embedded to drive a PPy based actuator. Figure 1 shows the conceptual design of the robotic fish that is developed in this project. The project is undertaken in collaboration with the Polymer Electronics Research Centre (PERC) at the University of Auckland.

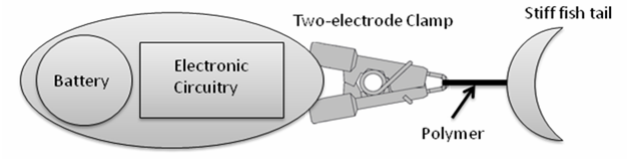


Figure 1: The conceptual design of the polymer actuated robotic fish, 9cm x 3.5cm x 1cm.

This report is organized as follow: Section 2 provides the theoretical background of CP actuation, focusing on the actuation of PPy films. Section 3 outlines the characterization process of the polymer actuator, which includes the experiment setup, experimental procedure and results. Section 4 describes the mechanical and electrical design choices for the prototype. Section 5 presents the implementation details of the prototype. Section 6 discusses the testing and evaluation. Concluding remarks and future work are discussed in Section 7.

## 2 Overview of Theory

CPs are a special class of organic materials featuring high electronic conductivities [Skotheim, Elsenbaumer et al. 1998]. All CPs have a conjugated structure, as depicted in Fig. 2.

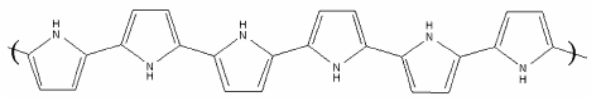

Figure 2: Structure of Polypyrrole (PPy)

The structure results in a delocalized positive charge when electrons are removed (oxidation) from the polymer by electrochemically applying a positive potential. To balance the charge neutrality, ions from surrounding electrolyte either enter or exit the polymer. It is this ion movement, accompanied by solvent, that is primarily responsible for the swelling or contraction of the material [Madden, Madden et al. 2001; Smela 2003; Madden and Vandesteeg 2004], as shown in Figure 3.

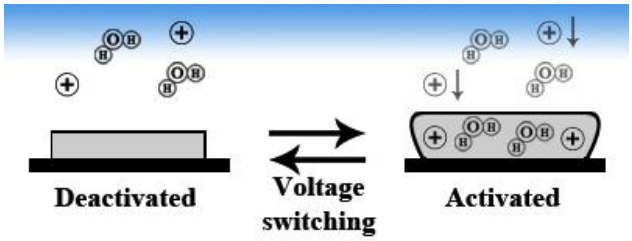


Figure 3: Oxidation and Reduction Process.

Previous literature states that the swelling and contraction of polymer could be closely related to the electrochemical redox processes occurring within the PPy [16]. The redox process is described by equation 1:

$$P^{+}(A^{-}) + C^{+} + e^{-} \longleftrightarrow P^{0}(AC) \qquad (1)$$

where *P+* represents the doped (oxidized) state of the polymer and $P^0$ the undoped (reduced, neutral) state. *P+(A-)* indicates that the anion *A-*, called the counter-ion, is incorporated into the polymer as a dopant, and $P^0(AC)$ indicates that a cation (co-ion) is inserted during reduction. The equation shows that to maintain charge balance, a change of electronic charge must be accompanied by an equivalent change of the ionic charge, which requires mass transport between polymer and electrolyte [Smela 2003].

## 3 Characterization of Actuators

CP actuator performance varies with different actuator configurations and different combinations of CPs and electrolytes. Analysis on these factors was required before proceeding further with robotic fish design. The design and production of CPs is still very much a research laboratory activity.

### 3.1 Actuator Configurations

The structure and composition of the PPy actuator considered in this project are shown in Figure 4:

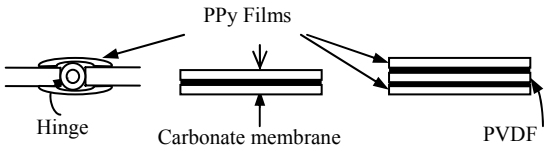


Figure 4: Actuator models, from left to right: linear strain model, bilayer model, trilayer model.

The linear strain model closely emulates the human joint. The film used in this configuration is a single layer, freestanding PPy film. The films function like human muscles around the joint. When stimulated, the films experience strain change, and hence, pull the moveable part of the actuator to generate force [Spinks and Campbell 2005]. In our case the fish tail is the moveable part of the actuator.

The bilayer and trilayer model are bending actuators. In a unimorph bilayer, a single film of PPy is polymerized onto a second inert layer. The actuator is then immersed into an aqueous electrolyte to enable ion exchange. A separate counter electrode is needed in this configuration. Electrochemically induced strain inside the polymer bends the bilayer actuator. There have been many actuator behavior experiments using this configuration, starting from 1992 [Smela 2003].

The trilayer or bimorph actuators have PPy films attached on both sides of inner passive films which are polyvinylidine fluoride (PVDF). PVDF is an electronically insulating porous film. It serves two purposes: it separates two PPy layers and it reserves electrolyte. PPy film on one side serves as a working electrode, the film on the other side acts as the counter electrode. The difference between the trilayer and bilayer configurations is that, the distance between the working and counter electrodes in the trilayer actuator is minimized. Thus, the actuations appear to be faster in trilayer actuators [Y.Wu, G.Alici et al. 2006].

### 3.2 Actuation behavior of different configurations

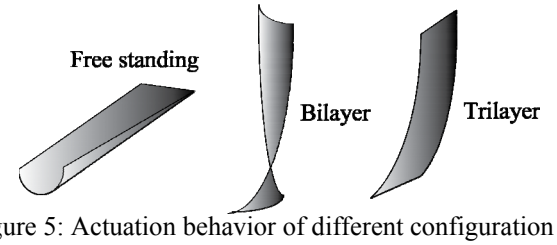


Figure 5: Actuation behavior of different configuration

As illustrated in Figure 5, freestanding film tends to curl

during actuation. Bilayer film often twists itself. The trilayer configuration shows the best actuation behavior because it is much more rigid compared to the other two configurations. Therefore, the trilayer is chosen as the configuration for the fish actuator. Further experiments are conducted based on this actuator configuration.

## 3.3 Experiments for Characterizing Actuators

**Reagent and Materials**

NaDBS (Sodium dodecylbenzene sulfonate, from Sigma-Aldrich Chemicals) in aqueous solution was used as received. Pyrrole (from Sigma-Aldrich) was distilled and stored under nitrogen at -20 $^{o}$C prior to use. The PVDF membrane, supplied by the University of Wollongong, was ~110 μm in thickness and was coated with a thin layer of gold on each side (~100 nm).

**Synthesis of PPy/DBS-Trilayer**

Polypyrrole (PPy) films were doped with dodecylbenzene sulfonate (DBS). Identical 5-20 μm PPy/DBS films were grown on both sides of the PVDF membrane to serve as working electrodes using galvanostatic (0.05 mA, 4$^{o}$C, 0.05 M pyrrole, 0.06 M NaDBS) polymerization using CH Instruments electro-chemical workstation, model 440 [Y.Wu, G.Alici et al. 2006; Kiefer, Paul A. Kilmartin et al. 2007]. As counter and reference electrode a Platinum-net was used.

**Apparatus Setup**

The experimental setup is shown in Figure 6. The eDAQ recorder (e-corder) in the centre, together with the potentiostat, are used to generate the desired electrical signal for each experiment. The Sony digital camera on the right is used to record the deflection of the actuator at 25 frames per second. The PC on the left records the video stream from the camera and displays the real-time signal from the e-corder. Other equipments include a metal stand, a two-electrode clamp and grid paper.

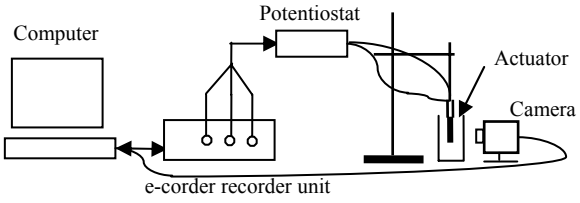


Figure 6: Experimental setup

**Experiment Procedure**

The produced trilayer actuator was immersed into 0.2 mol/L TMACl (Tetramethylammonium chloride) or NaCl (0.1 mol/L ~ 0.5 mol/L) solution. A 50% duty cycle square wave was used to cycle the trilayer at a range of frequencies (0.03Hz ~ 10Hz) with a potential level of 0.8V. The movement of the trilayer was recorded using the camera. Individual frames were captured from the recorded video stream using the ImageGrab software package. Figure 7 shows two example images. Software was written to calculate the deflection of the actuator as a function of time. A graphical user interface assists the experimenter to process the images.

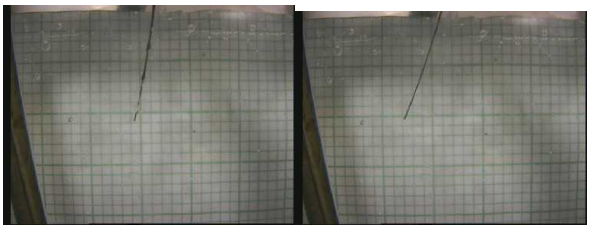

Figure 7: Sample images captured during the experiment

## 3.4. Results Discussion

The following properties of the actuator are obtained from the experimental results:

**Deflection versus time**

Figure 8 illustrates a typical experiment plot of actuator deflection. The y-axis represents the amount of deflection at different points of the actuator. In this case, the tip of the actuator (2.5 cm from the fixed end) gives the largest displacement of 3.3 mm from its original position. The x-axis represents time. This particular experiment uses a cycling frequency of 0.03 Hz. The whole experiment lasts 150 seconds. From the graph, it is clear to see that the actuator experiences three peak displacements with different peak values. This implies that there is a drift inside this actuator, i.e. the actuator does not return to its starting position after one complete cycle of operation.

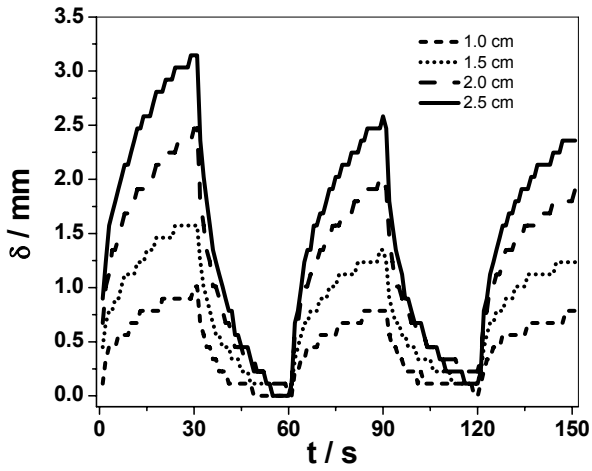


Figure 8: Deflection δ of the PPy/DBS-Trilayer (Thickness PPy: 15 μm, Thickness PVDF: 110 μm, length 2.5 cm, width: 2 mm) at different areas of the Trilayer (from top to bottom: 2.5 cm, 2.0 cm, 1.5 cm, 1.0 cm).

**Force estimation**

The force required to actuate the polymer can be approximated using Hook's law:

$$F = \frac{\delta \cdot a \cdot b^2 \cdot E}{4 \cdot L^3} \qquad (2)$$

where $\delta$ is the displacement; $a$ is the width of the actuator; $b$ is the thickness of the actuator; $E$ is the estimated Young's modulus; $L$ is the length of the actuator.

Using formula (2), the forces needed at different points of

the actuator from experiment result as shown by Figure 8 are calculated. The results are shown in Figure 9. In conclusion, a shorter actuator needs a stronger force to bend it. This is why the 1.0 cm curve appears above all the other curves in Figure 9.

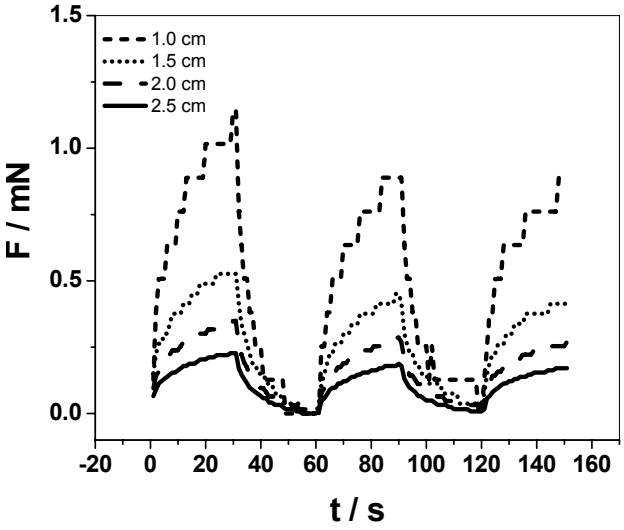


Figure 9: Force F of the PPy/DBS-Trilayer (Thickness PPy: 15 µm, Thickness PVDF: 110 µm, length 2.5 cm, width: 2 mm) at different areas of the Trilayer (from top to bottom: 1.0 cm, 1.5 cm, 2.0 cm, 2.5 cm).

**Thickness versus frequency**

Figure 10 plots the deflection versus frequency curve for the polymers with different thicknesses. It is showed that the 10µm PPy film gives the best actuation at all frequencies. At 1 Hz, especially, the deflection is measured to be around 4 mm for a 2.5 cm PPy trilayer.

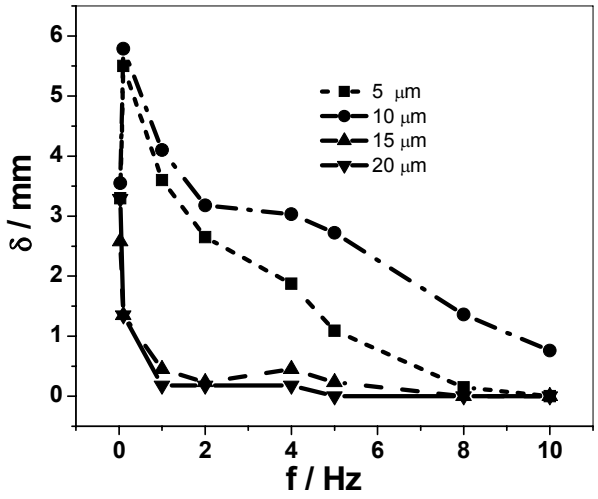


Figure 10: Thickness (-■- 5 µm, -●-10 µm, -▲- 15 µm and -▼- 20 µm) of PPy/DBS layers on PVDF Trilayer with length of 2.5 cm in dependence of the frequency (0.03 Hz- 10 Hz).

To summarize the findings from the experiments, it is discovered that the deflection of an actuator tends to increase as the actuator length increases. The amount of force that an actuator needs to bend is inversely proportional to its length. The actuator shows the best actuation at around 1 Hz. The 10 µm PPy film gives the largest displacement among all tested thicknesses. It is, therefore, decided to choose the following parameters to design the fish actuator:

- 10 µm thick PPy film synthesized on PVDF
- 2.5 cm in length
- Stimulated with 1Hz square wave.
- NaCl solution.

## 4 A Polymer Actuated Robot Fish

The findings from the previous section lead to the fish design specifications below. It is also necessary for the designed robotic fish to:

- Have a minimized size and weight.
- Have neutral buoyancy.
- Be self-powered.
- Work with a PPy actuator.

### 4.1. Mechanical Design

The two basic factors that are considered during mechanical design are: (i) the shape and location of propulsors; (ii) movement pattern [Colgate and Lynch 2004]. Fish swimming modes are tightly related to these factors. Fish that generate thrust using body and caudal fin motions are known as BCF swimmers. Other Fish that generate thrust using median (dorsal or anal) and paired fins, are classified MPF swimmers.

Figure 11: Example of BCF propulsion fish on the left and MPF propulsion fish on the right. Shaded areas generate thrust. Modified from [Colgate and Lynch 2004]

The robotic fish implements the BCF swimming model for two reasons. Firstly, BCF swimmers exhibit good efficiency at reasonably high speeds in nature [Colgate and Lynch 2004]. Secondly, to the extent of our knowledge, there has been no robotic fish based on a PPy actuator with this configuration.

**Thrust Generation and Tail Model**

The forward thrust generated by tail propulsion is mainly from following four factors: (i) High aspect ratio of caudal fins; (ii) a curved leading edge of tail; (iii) stiff fins; (iv) the oscillatory motion of the fins [Sfakiotakis and Lane 1999]. The implemented actuator fulfills all these four criteria.

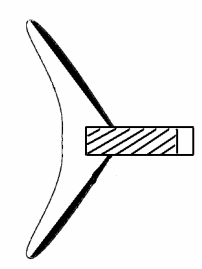

Figure 12: Design of PPy actuator.

The initial approach considered was to encapsulate the PPy film with very thin insulating films. Previous work reported that this would result in a much stiffer actuator. However, it was found under observation that this method greatly reduced the amplitude of actuation. Therefore, trilayer PPy actuators with no encapsulation were used in actuator design.

The other advantage of using trilayer PPy films was that they were capable of working in an aqueous solution, such as NaCl or even sea water. This was very important for minimizing the cost. For example, 1 liter of 0.2 M TMACl solution costs around USD$300. In contrast, NaCl solution (sea water) can be obtained at nearly zero cost. Secondly, TMACl solution is toxic if dumped into the environment. NaCl, on the other side, is eco-friendly.

**Fish Body Design and Packaging**

The fish body design is the key to minimizing hydraulic drag force. The packaging also needs to be waterproof to protect all the electronics onboard, yet provide access to replace the battery and to program the Atmel micro-controller.

One way of packaging was to place the PCB inside a case, and sealed the case with silicon adhesive. Another design option was to fabricate a mould for the fish. The mould is then painted with liquid rubber for sealing. This method has been experimented with at the Michigan State University [Tan, Kim et al. 2006]. The feedback was that the painting of rubber skin must be done multiple times in order to prevent leaking. This method was not considered reliable enough. Thus, it was decided to use a plastic case as the fish body and seal it with silicone gel. The case used was a fish shape plastic shell. It fits the circuit board perfectly in size, and is very light. The sealed case had been tested and does not leak.

## 4.2. Electronics Design

PCB circuitry is needed to reproduce the working condition of the polymer actuator. The following design parameters are written into the hardware design specification. The hardware needs to:

- Be able to supply a 50 % duty cycle square wave switching between 0.8 V and -0.8 V at variable frequency (1 Hz by default).
- Be able to supply at least 30 mA to the output port, such that multiple actuators could be operated at the same time.
- Be as small and as light as possible, in order to minimize the size and weight of the robotic fish.
- Be upgradable. Future expansion of the current circuit should be possible.

A system diagram of the designed PCB is shown in Figure 13.

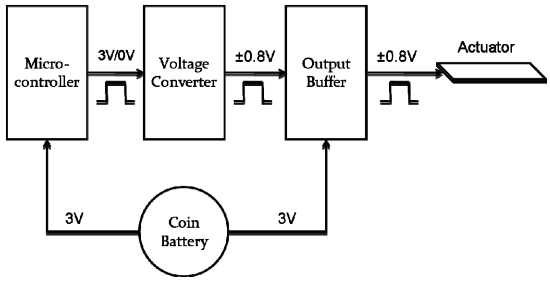


Figure 13: System diagram of the PCB circuit

**Approaches to power the robotic fish**

The specification states that the fish is self-contained. This excludes the possibility of powering the robotic fish through wires from off-robot sources. It would be nice to power the fish wirelessly using inductive power transfer (IPT). However, this approach has two drawbacks. Firstly, it limits the working range of robotic fish to a confined area (only where the IPT power source is applicable). Secondly, it requires the fish to have a large coil for power pickup, and thus increases the weight and size. Therefore, the only feasible option for a power source is onboard batteries. Many types of batteries have been investigated.

Conventional alkaline batteries are heavy and bulky. Zinc-air batteries (used for hearing aids) require oxygen to function, which is not available when working under water. Lithium coin cell batteries have an excellent capacity-to-size ratio and were chosen as the power source in our prototype.

**Approaches to generate output signals**

The required signal to drive the PPy actuator is a 50 % duty cycle square wave with peak value of 0.8 V. The optimal frequency to operate the actuator is 1Hz. This section described the approaches we have considered during the design process.

The simplest approach is a voltage divider for lowering the input voltage to the actuation voltage. However, the problem with this approach is that the input voltage from battery is not constant. As the battery drains, the output voltage of the battery tends to decrease. Therefore, this approach cannot guarantee a constant voltage supply to the actuator.

Another idea is a voltage reference. The simplest form of voltage reference is a zener diode [Horowitz 1980]. However, a search in common electronics suppliers did not return any zener diode with the desired breakdown voltage.

Another popular voltage reference is the band-gap reference. The band-gap voltage reference features extremely low power drain and good temperature stability. Typical operating range of such diodes is from 1.2 V to 5.3 V. The band-gap voltage reference is available in two configurations: a normal configuration which gives a pre-defined output voltage level, and an adjustable configuration, the output can be adjusted to any voltage within the working range. In this case, both configurations are used.

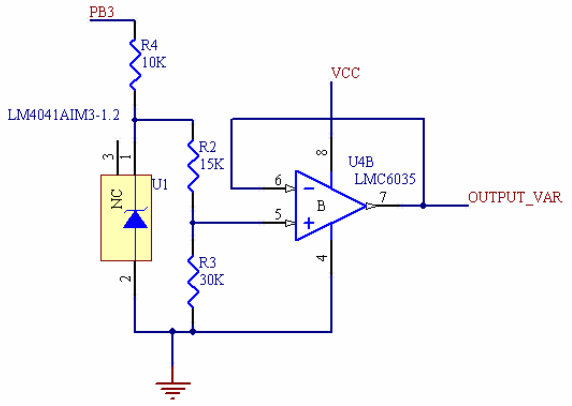


Figure 14: Application of the LM4041-1.2 voltage reference.

Figure 14 shows the application of the LM4041-1.2 band-gap voltage reference in the normal configuration. An external series resistor R4 was connected between the supply voltage and the LM4041. R4 determines the current that flows through the voltage reference and load. The value of R4 was selected based on the supply voltage, ($V_S$), the desired load and operating current, ($I_L$ and $I_Q$), and LM4041-1.2 reverse breakdown voltage, $V_R$.

$$R_S = \frac{V_S - V_R}{I_L + I_Q} \tag{3}$$

Resistors R2 and R3 formed a voltage divider which scaled the 1.225 V from voltage reference down to 0.8 V.

In Figure 15, the band-gap voltage reference was used in adjustable mode. The output voltage was determined using the formula as shown in equation 3:

$$V_O = V_{REF} \times (\frac{R_6}{R_5} + 1) \tag{4}$$

In this case, an output voltage of 1.6 V was generated using the configuration shown in Figure 15.

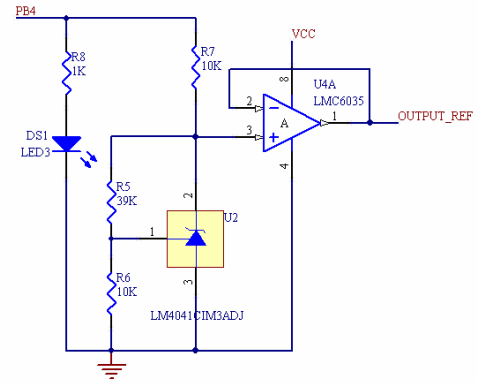


Figure 15: Application of LM4041-ADJ voltage reference

**Microcontroller**

A microcontroller was used to either switch on the circuit in Figure 15 to output a voltage of 1.6V, or switch it off to output 0V. This could be achieved by periodically switching on/off the output pin of the microcontroller. Alternatively, a PWM signal could be used. The decision on which microcontroller to use was made based on the availability of the toolkit and the amount of support available.

The ATMEL ATtiny series of microcontrollers was used. The ATtiny2313 microcontroller is a very powerful chip with four PWM channels. It was supported with a full suite of program and system development tools including: C Compilers, Macro Assemblers, Program Debugger Simulators, In-Circuit Emulators, and Evaluation kits. Although many features on the ATtiny chip were not used at this stage of the project, the choice of ATtiny2313 made any future upgrade to the circuit very convenient.

It was considered that closed loop control circuitry was not necessary for the scope of this project. Therefore, there was no feedback sensor integrated into the current circuitry.

**Two-electrode clamp**

A two-electrode clamp, shown in Figure 16, was used to hold the polymer actuator in place and deliver the actuating signal to the polymer. Platinum pads were soldered onto the gold-plated tips of the clamp to improve conductivity between the clamp and the actuator.

Figure 16: Hirschmann Micro SMD test clip (adapted from RS Components NZ)

**Magnet Switch**

A magnetic reed switch (shown in Figure 17) was used to turn on the circuit. This prevented the potential leaking problem caused by installing other types of switches, such as a push button switch.

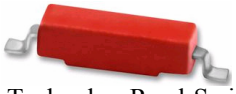

Figure 17: COTO Technolgy Reed Switch (adapted from Farnell Components NZ).

## 5. Implementation

This section describes the implementation details of the robotic fish prototype, shown in Figure 18.

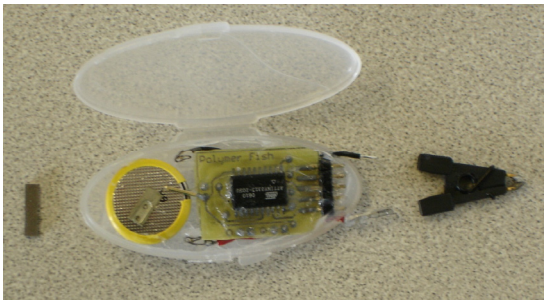

Figure 18: Pictorial view of the robotic fish (9.7 cm long, 3.5 cm wide, 1 cm thick, plus a tail of approx 2.5 cm).

The prototype consisted of the following parts:

- one 3 V lithium cell battery
- a fully assembled PCB circuit board
- a two-electrode clamp

- a small piece of magnet
- a plastic shell

### 5.1. The STK500 board

The STK500 board shown in Figure 19 was used to program the microcontroller. It has a 10-pin ISP header which is used specifically for programming external devices.

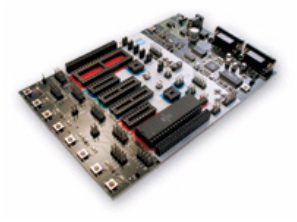

Figure 19: Atmel AVR STK500 development board [Adapted from STK500 handbook].

Embedded C code was written and compiled in AVR Studio 4. The generated hex code was downloaded onto the ATtiny2313 microcontroller via a 10-wire ribbon cable using the STK500 board. Alternatively, a programmer called donkey, which was recently designed by the ECE department, could be used to program the chip on the robotic fish.

### 5.2. Circuit assembly

The PCB was manufactured using the ECE department PCB mill. The ATTiny microcontroller was placed on one side of the PCB. Other surface mounted components were soldered on the other side of the board. An LED was used to indicate the working status of the system. A single-pole single-throw type reed switch was used so that when the switch was open, the whole circuit would be switched off. The output channels (PB3) controlled the circuit shown in Figure 14. PB3 was always set to logic high. This gives a constant 0.8 V offset at the output_ref terminal. In Figure 15, The PWM channel (PB4) generated a 50 % duty cycle square wave. This made the voltage output from the output_var terminal switching between 1.6 V and 0 V. The voltage difference from the two output terminals was therefore a signal switching between 0.8 V and -0.8 V.

### 5.3. Fish body assembly

A lithium coin battery was placed at the front end of the plastic case. The circuit board had its corners trimmed and was fitted at the rear end of the case. The battery was connected to the circuit board using two metal pins. Two output terminals extended out the case through holes drilled at the rear end. The two-electrode clamp was connected to the output terminals at the rear of the fish body.

The entire fish body was sealed with silicone gel as well as the connections between clamp and terminals. The fish was kept in a cool and dry place for 24 hours before the fish was tested in the solution. The silicone gel formed a complete insulation layer around the case, which could be easily peeled off as needed.

## 6. Testing and evaluation

In order to evaluate the performance of the robotic fish, testing on actuators was carried out in both TMACl and NaCl solution in a small container. The motion of the actuator was recorded using a digital camera. The Recorded images were analyzed using MATLAB software to read out the actuator displacement and speed. The prototype was tested in a large water tank filled with 0.2 M NaCl solution. TMACl solution was not used for large scale testing due to its high cost.

### 6.1. Prototype Lifetime

Lifetime of both the prototype and polymer actuator was tested. The prototype was powered by a standard 200mAh CR2302 lithium battery. The designed fish prototype was able to swim for at least 10 hours in an NaCl solution. The lifetime of the prototype was limited by the battery capacity. After 10-hours of operation, the microcontroller stopped due to the battery voltage dropping below the working range. The durability of the PPy polymer actuator was also tested. Results showed that the PPy polymer actuator was capable of continuous operation for at least 24 hours.

### 6.2. The reduced frequency or Strouhal number

The Strouhal number is defined by:

$$St = \frac{fA}{U} \tag{5}$$

where $f$ is the tail-beat frequency, $A$ is the tail-beat peak-peak amplitude, $U$ is the average forward velocity. The Strouhal number represents the ratio of unsteady to inertial force. Triantafyllou et.al point out that St is in the range of 0.25 ~ 0.40 for an efficient design [Triantafyllou and Triantafyllou 1995]. The Strouhal number of the prototype developed in this project is estimated to be around 4, which means that the robotic fish needs to increase its velocity by more than 10 times in order to achieve the efficiency of a natural fish.

### 6.3. Actuator Performance

The actuator was subjected to long-term testing to measure its performance. An interesting actuation pattern of the PPy polymer actuators was found, as illustrated in Figures 20a and b.

In Figure 20a, the PPy/DBS trilayer actuator was tested in TMACl solution. The deflection at 2.5cm point of the trilayer showed an increase of +80% in deflection amplitude from step 1 to step 30000. (1 step = 1 second). Further cycling showed a decrease of deflection amplitude until step 43000. This tendency, an increase followed by a decrease of the Trilayer deflection, was also observed in the NaCl electrolyte (Fig 20b).

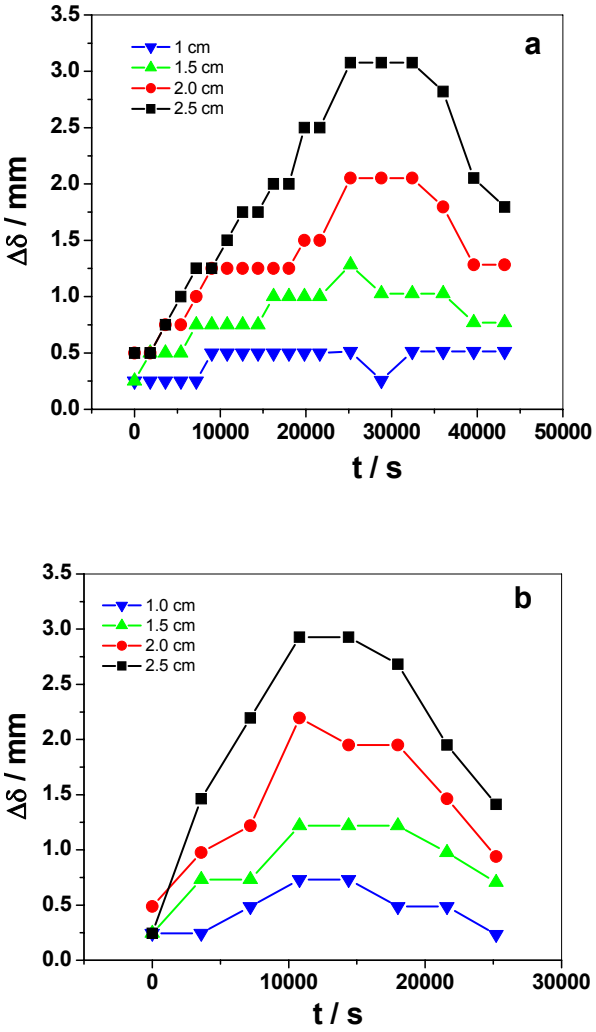


Figure 20: PPy/DBS Trilayer (thickness PPy: 10 µm, length 2.5 cm, width: 2mm) in a: TMACl (0.2 M ) and b: NaCl (0.2 M) cycled with 1 Hz/step between 0.8 V and -0.8 V controlled over the electronic fish device. The deflection of the Trilayer was observed at different points (-■- 2.5 cm, -●- 2.0 cm, -▲- 1.5 cm and -▼- 1.0 cm).

This unexpected behaviour of the PPy/DBS Trilayer actuator could possibly be explained with the study of the charging and discharging behaviour of PPy films. In our case, the actuation of polymer was determined by solvated cations (TMA+ or Na+) at reduction. Ion channels related to the size of the cations are formed during charging and discharging. The increasing of actuator deflection could be due to the process of slow penetration of the cations (TMA+) by a diffusion mechanism inside the PPy film. The bigger the cations' size, the longer the cations took to penetrate the PPy layer. Therefore, for a smaller cation, such as Na+, the penetration seemed faster.

This example clearly shows the complexity of PPy actuation mechanism. In order to gain a better control over the actuator behaviour, a full understanding of the actuation mechanism must be obtained. However, no formal theory of polymer actuation mechanism has been established up to now. This subject is still a research in progress.

The displacement and speed of actuator can be derived from Figure 20. The result is shown in Table 1. The designed actuators worked well in both TMACl and NaCl solutions in terms of displacement and speed. The actuation in TMACl solutions showed a slightly larger displacement due to the larger size of TMA+ ions. The maximum oscillation speeds of the actuators in both solutions were similar. It was 2.8mm/s in TMACl and 2.9 mm/s in NaCl.

Table 1: Displacement and Speed of Actuator in TMACl and NaCl solutions(0.2mol/L)

| Time (sec) | TMACl | | NaCl | |
|---|---|---|---|---|
| | Displacement (mm) | Speed (mm/s) | Displacement (mm) | Speed (mm/s) |
| 2000 | 0.5 | 3 | 1.48 | 1.4 |
| 10000 | 1.5 | 2.2 | 2.9 | 2.9 |
| 20000 | 2.5 | 2 | 2 | 2 |
| 30000 | 3.1 | 2.8 | - | - |
| 40000 | 2.1 | 1.9 | - | - |

## 7. Future works

On the actuator side, future work will include further collaboration with the chemistry department, especially the Polymer Electronic Research Centre. More research efforts will be made to synthesize better polymers with stronger and larger actuation. We expect this to be possible since there are polymers with better performance, however this is still very much a research area.

Electronically, a more sophisticated control scheme will be implemented in the robotic fish. Turning and diving of the fish can be realized in the future. At the same time, some sensors (visual, ultrasonic and infrared detectors) are planned to be implemented into the fish body, so that the robotic fish is able to react to the change in the environment and have certain local autonomy.

## 8. Conclusions

In this paper, the development of a robotic fish based on a polymer actuator is reported. The fish used a PPy based actuator to generate swimming motions. Extensive experiments were conducted to characterize the behavior of PPy films. Actuators based on the shape of a caudal fin were designed. The robot was powered by a Lithium coin battery and was completely self-contained. Waterproof packaging was designed to protect the electronics inside. This is the first time such a project has been undertaken in the world. As a proof-of-concept, this project successfully shows a working prototype with 10-12 hours lifetime with an average speed of 1-2 mm/s. It is concluded that the weak actuation of PPy material was the major limitation of the prototype.

## Acknowledgements

This project was supported in conjoint by Electrical and Computer Engineering (ECE) and the Electronic Polymer Research Centre (PERC) at the University of Auckland. The authors would like to thank the technical staff of both departments for providing the support and guidelines to make this project successful. We appreciated the assistance of Gursel Alici and Geoffery Spinks from the University of Wollongong, who supplied the PVDF films.

## References


[Alici, G. and G. Spinks 2006] Alici, G. and G. Spinks. Establishment of a Biomimetic Device Based on Tri-layer Polymer Actuators - Propusion Fins. NSW, Australia, University of Wollongong.

[Bandyopadhyay, P. R. 2005] Bandyopadhyay, P. R. "Trends in Biorobotic Autonomous Undersea Vehicles." IEEE Journal of Oceanic Engineering 30(1): 109-140.

[Bar-Cohen, Y. 2001] Bar-Cohen, Y. Electroactive polymer (EAP) actuators as artificial muscles. Bellingham, Washington, SPIE Press.

[Bar-Cohen, Y. 2004] Bar-Cohen, Y. "Electroactive Polymers as actuators for potential future planetary mechanisms." Proceedings of the 2004 NASA DOD conference on Evolution Hardware.

[Colgate, J. E. and K. M. Lynch 2004] Colgate, J. E. and K. M. Lynch. "Mechanics and Control of Swimming: A Review." IEEE Journal of Oceanic Engineering 29(3): 660-674.

[Edd, J., S. Payen, et al. 2003] Edd, J., S. Payen, et al. Biomimetic Propulsion for a Swimming Surgical Micro-Robot. Proceedinas of IEEE/IRSI lnternational ConfGence on Intelhginl Robots and Systems, Los Angles, Nevada.

[Horowitz, P. 1980] Horowitz, P. The Art of Electronics, Cambridge University Press.

[Kiefer, R., Paul A. Kilmartin, et al. 2007] Kiefer, R., Paul A. Kilmartin, et al. "Actuation of polypyrrole film in propylene carbonate electrolytes." Sensors and Actuators.

[Leonard, N. E. and J. G. Graver 2001] Leonard, N. E. and J. G. Graver. "Model-Based Feedback Control of Autonomous Underwater Gliders." IEEE Journal of Oceanic Engineering 26(4): 633-645.

[Madden, J. D. W., P. G. A. Madden, et al. 2001] Madden, J. D. W., P. G. A. Madden, et al. Polypyrrole actuators: modeling and performance. Electroactive Polymer Actuators and Devices,. Newport Beach, CA.

[Madden, J. D. W. and N. A. Vandesteeg 2004] Madden, J. D. W. and N. A. Vandesteeg. "Artificial Muscle Technology: Physical Principles and Navel Prospects." IEEE Journal of Oceanic Engineering 29(3): 706.

[Punning, A., M. Anton, et al. 2004] Punning, A., M. Anton, et al. A Biologically Inspired Ray-like Underwater Robot with Electroactive Polymer Pectoral Fins.

[Reynolds, J. R. 2006] Reynolds, J. R. Artificial Muscles. Conjugated Polymer Processing and Applications, CRC Press: 591.

[Sfakiotakis, M. and D. M. Lane 1999] Sfakiotakis, M. and D. M. Lane. "Review of Fish Swimming Modes for Aquatic Locomotion." IEEE Journal of Oceanic Engineering 24(2): 237-253.

[Skotheim, T. A., R. L. Elsenbaumer, et al. 1998] Skotheim, T. A., R. L. Elsenbaumer, et al. Handbook of Conducting Polymers. Marcel Dekker, New York.

[Smela, E. 2003] Smela, E. "Conjugated Polymer Actuators for Biomedical Applications." Advanced Materials 15: 481.

[Spinks, G. M. and T. E. Campbell 2005] Spinks, G. M. and T. E. Campbell. "Force generation from polypyrrole actuators." Smart Materials and Structures 14: 406-412.

[Spinks, G. M., L. Liu, et al. 2002] Spinks, G. M., L. Liu, et al. "Strain Response from Polypyrrole Actuators under Load." Advanced Functional Materials 6: 437.

[Tan, X., D. Kim, et al. 2006] Tan, X., D. Kim, et al. An Autonomous Robotic Fish for Mobile Sensing. International Conference on Intelligent Robots and Systems, Beijing,China.

[Triantafyllou, M. S. and G. S. Triantafyllou 1995] Triantafyllou, M. S. and G. S. Triantafyllou. "An efficient swimming machine." Science American: 64-70.

[Y.Wu, G.Alici, et al. 2006] Y.Wu, G.Alici, et al. "Fast trilayer polypyrrole bending actuators for high speed applications." Synthetic Metals 156: 1017-1022.